

Phases of QCD at nonzero isospin and strangeness chemical potentials with application to pion stars

Jens O. Andersen, Martin Kjøllestadal Johnsrud

Department of Physics, Norwegian University of Science and Technology, Høgskoleringen 5, Trondheim, N-7491, Norway

Abstract

We study pion and kaon condensation using three-flavor chiral perturbation theory at finite isospin and strangeness quark chemical potentials μ_I and μ_S . The phase diagram consists of a vacuum phase and three distinct Bose condensed phases with condensates of charged pions as well as charged and neutral kaons. Adding electromagnetic interactions, a phase with a charged condensate becomes a Higgs phase and the resulting phase diagram is modified due to the electromagnetic mass splittings of the mesons. The results for the pion-condensed phase are applied to calculate mass-radius relation of pion stars. Local electric charge neutrality is imposed by adding electrons, muons together with their neutrinos. Finally, we compare our results for the mass-radius relations with those from recent lattice simulations, and find very good agreement.

Keywords: QCD phase diagram, chiral perturbation theory, meson condensation, compact stars

1. Introduction

The phase diagram of quantum chromodynamics (QCD) has received a lot of attention since the first sketchy version of it appeared in the 1970s. At the time, it was expected that it consists of two phases, a hadronic phase at low temperature and small baryon chemical potential μ_B , and a deconfined phase at high temperature and/or large baryon chemical potential. In 1984, Bailin and Love [1] suggested that QCD at large baryon chemical potential is a color superconductor. The result is based on the fact that there is an attracting channel in the one-gluon exchange diagram in QCD and that perturbation QCD is valid for large μ_B due to asymptotic freedom. This renders the Fermi surface unstable and in analogy with BCS theory leads to the formation of Cooper pairs. Since then a number of colors-superconducting phases have been found whose exact location is model dependent. See Refs. [2, 3, 4] for reviews.

Conventionally, the QCD phase diagram has been drawn in the μ_B - T plane, but we can add more axes to it, for example by allowing for an independent quark chemical potential μ_f for each flavor f . For two flavors, this implies that we introduce an isospin chemical potential μ_I and for three flavors an additional strangeness chemical potential μ_S . The new μ_I - T plane has received particular attention, in part by the fact that fermion determinant in QCD at finite isospin density and zero baryon and strangeness density is real, which implies that the system is free of

the sign problem. Thus one can carry out lattice simulations using standard importance sampling techniques and study pion condensation and the transition line in the μ_I - T plane. The first lattice simulations carried out more than 20 years ago [5, 6, 7, 8, 9] suggested that the phase transition is second order with critical exponent from the $O(2)$ universality class. At zero temperature the transition takes place at $\mu_I = m_\pi$, which is expected for a second-order phase transition. In recent years, high precision lattice simulations have been carried out confirming the second-order nature of the transition at $T = 0$. Moreover, quark and pion condensates as functions of μ_I were obtained [10, 11, 12, 13].

Condensation of pions, kaons, and diquarks in QCD and QCD-like theories has also been studied using chiral perturbation theory (χ PT) [19, 20, 21, 22, 23, 24, 25, 26, 27]. χ PT is an effective low-energy theory based on the global symmetries and relevant degrees of freedom of the the fundamental theory (QCD or QCD-like) [28, 29]. The second-order nature of the transition at low temperatures, where χ PT is valid, as well as the critical chemical potential being equal to the mass of the condensing particle (at $T = 0$) were confirmed.¹ Finally, excellent agreement between lattice and $\mathcal{O}(p^4)$ result in chiral perturbation for the quark and pion condensates at $T = 0$ was found. A recent review of meson condensation can be found in Ref. [30].

In Ref. [31], the authors considered the problem of pion condensation in a dense neutrino gas. At $T = 0$, it was

Email addresses: andersen@tf.phys.ntnu.no (Jens O. Andersen), martkjoh@stud.ntnu.no (Martin Kjøllestadal Johnsrud)

¹This has been shown at order $\mathcal{O}(p^2)$ and $\mathcal{O}(p^4)$ in the low-energy expansion of χ PT and is expected to hold to all orders.

shown that for sufficiently large neutrino chemical potentials and therefore neutrino densities, a charged pion condensate is formed in electrically neutral matter in chemical equilibrium. The electron and muon provide the background electric charge that neutralizes the charged pion condensate. This opens up the possibility to probe the QCD phase diagram if these conditions are met, for example in the early universe. This question was addressed in Refs. [15, 16, 17]. In Ref. [17], the authors use an HRG model where the pion contribution is replaced by an interacting pion gas based on lattice simulations [18], to allow for pion condensation. The resulting pressure is parameterized by the temperature T and five different chemical potentials, corresponding to the conserved charges B , Q , and the three lepton numbers. Given that the baryon and electric charge per entropy ratios are tightly constrained, the cosmic trajectories can be parameterized by the lepton asymmetries $l_{e,\mu,\tau}$. While the sum of them is tightly constrained, the individual contributions are not. By varying $l_e + l_\mu$ with $l_e = l_\mu$ and $l_e + l_\mu + l_\tau = 0$, different cosmic trajectories are obtained. For lepton asymmetry $l_e + l_\mu = 0.1$ or larger, the trajectories enter the pion condensed phase in the μ_Q - T plane, where the transition line was obtained from lattice calculations [18]. The idea of a pion star formed by a Bose condensate of charged pions was first suggested in Ref. [24]. A detailed study of their properties, with and without charge neutrality constraint, based on an EoS from lattice simulations of QCD at finite isospin density, can be found in Ref. [14].

In this paper, we continue the study of pion and kaon condensation in the context of χ PT, including electromagnetic effects. We apply the results for pion condensation to pion stars. A detailed analysis will be presented elsewhere [32], see also [33]. The letter is organized as follows. In Sec. 2, we briefly discuss the chiral Lagrangian at finite chemical potentials and map out the phase diagram at $T = 0$ in the μ_I - μ_S plane including electromagnetic effects. In Sec. 3, we discuss pion stars at finite isospin chemical potential. We discuss the nonrelativistic and Newtonian limits as well as the effects of imposing local charge neutrality. The mass-radius relation is calculated and we compare our results with those of recent lattice simulations.

2. Phases of QCD at nonzero μ_I and μ_S

The original formulation of chiral perturbation theory by Gasser and Leutwyler was in the strong sector [28, 29]. Later, electromagnetic interactions were included by Ecker et al. [34] at $\mathcal{O}(p^2)$, and by Urech [35, 36] and by Meissner et al. [37] at order $\mathcal{O}(p^4)$. In the presence of electromagnetic interactions, the $\mathcal{O}(p^2)$ chiral Lagrangian for

three-flavor QCD is

$$\begin{aligned} \mathcal{L}_2 = & -\frac{1}{4}F_{\mu\nu}F^{\mu\nu} + \frac{1}{4}f^2\langle\nabla_\mu\Sigma\nabla^\mu\Sigma^\dagger\rangle \\ & + \frac{1}{4}f^2\langle\chi^\dagger\Sigma + \Sigma^\dagger\chi\rangle + C\langle Q\Sigma Q\Sigma^\dagger\rangle \\ & + \mathcal{L}_{\text{gf}} + \mathcal{L}_{\text{ghost}}, \end{aligned} \quad (1)$$

where $\langle A \rangle$ means the trace of the matrix A , $F_{\mu\nu}$ is the electromagnetic field tensor, $\nabla_\mu\Sigma = \partial_\mu\Sigma - i[v_\mu - A_\mu Q, \Sigma]$ is the covariant derivative, $\chi = 2B_0\text{diag}(m_u, m_d, m_s)$, $Q = e\text{diag}(\frac{2}{3}, -\frac{1}{3}, -\frac{1}{3})$ is the charge matrix, f is the bare pion (or kaon) decay constant, and C is a constant that determines the electromagnetic mass splittings at tree level. \mathcal{L}_{gf} and $\mathcal{L}_{\text{ghost}}$ are the ghost and gauge-fixing terms in the chiral Lagrangian, but their expressions are not needed in this letter. Finally, Σ is the standard parameterization of the Goldstone fields,

$$\Sigma = \exp\left[\frac{i\lambda_a\phi_a}{f}\right], \quad (2)$$

where λ_a are the Gell-Mann matrices and $v_\mu = v_0\delta_{\mu 0}$ with

$$v_0 = \frac{1}{3}(\mu_B - \mu_S)\mathbb{1} + \frac{1}{2}\mu_I\lambda_3 + \frac{1}{\sqrt{3}}\mu_S\lambda_8, \quad (3)$$

where the baryon, isospin, and strangeness chemical potentials expressed in terms of the three quark chemical potentials μ_f are

$$\mu_B = \frac{3}{2}(\mu_u + \mu_d), \quad (4)$$

$$\mu_I = (\mu_u - \mu_d), \quad (5)$$

$$\mu_S = \frac{1}{2}(\mu_u + \mu_d - 2\mu_s). \quad (6)$$

Alternatively, if we introduce the chemical potentials $\mu_{K^\pm} = \frac{1}{2}\mu_I + \mu_S$ and $\mu_{K^0} = -\frac{1}{2}\mu_I + \mu_S$, we can write

$$v_0 = \frac{1}{3}(\mu_B - \mu_S)\mathbb{1} + \frac{1}{2}\mu_{K^\pm}\lambda_Q + \frac{1}{2}\mu_{K^0}\lambda_K, \quad (7)$$

where $\lambda_Q = \lambda_3 + \frac{1}{\sqrt{3}}\lambda_8$ and $\lambda_K = -\lambda_3 + \frac{1}{\sqrt{3}}\lambda_8$. Note that $\{\lambda_4, \lambda_5, \lambda_Q\}$ and $\{\lambda_6, \lambda_7, \lambda_K\}$ form the remaining two $SU(2)$ algebras of $SU(3)$. After having introduced the chemical potentials, the symmetry is reduced to $U(1)_I \times U(1)_Y$ or equivalently $U(1)_Q \times U(1)_K$. In the absence of electromagnetic interaction, these are global symmetries. Including them, the $U(1)_Q$ symmetry is being gauged and is thus local. Since the unit operator commutes with all the generators of $SU(3)$, the results will be independent of μ_B , which simply reflects that the mesons have zero baryon number and that Σ is a singlet under $U(1)_B$ transformations.

By expanding the Lagrangian Eq. (1) with vanishing chemical potentials to second order in the fields ϕ_a , we can read off the tree-level meson masses in the vacuum. Considering first the case without EM contributions, we

have

$$m_{\pi^0}^2 = m_{\pi^\pm,0}^2 = B_0(m_u + m_d), \quad (8)$$

$$m_{K^\pm,0}^2 = B_0(m_u + m_s), \quad (9)$$

$$m_{K^0/\bar{K}^0}^2 = B_0(m_d + m_s), \quad (10)$$

$$m_\eta^2 = \frac{1}{3}B_0(m_u + m_d + 4m_s). \quad (11)$$

Including EM contributions, the masses of the charged particles become

$$m_{\pi^\pm}^2 = m_{\pi^\pm,0}^2 + \Delta m_{\text{EM}}^2, \quad (12)$$

$$m_{K^\pm}^2 = m_{K^\pm,0}^2 + \Delta m_{\text{EM}}^2, \quad (13)$$

where $\Delta m_{\text{EM}}^2 = 2C \frac{e^2}{f^2}$.

In order to understand the phase diagram in three-flavor QCD, it may be useful to first take a look at the two-flavor case and pion condensation. In this case $v_0 = \frac{1}{3}\mu_B \mathbb{1} + \frac{1}{2}\mu_I \tau_3$, where τ_a are the Pauli matrices. For $\mu_I = 0$, the vacuum state Σ_0 is given by the 2×2 unit matrix, $\Sigma_0 = \mathbb{1}$. For finite μ_I , the most general ansatz for the ground state is [19, 20]

$$\Sigma_\alpha^{\pi^\pm} = \cos \alpha \mathbb{1} + i \hat{\phi}_a \tau_a \sin \alpha, \quad (14)$$

where $\hat{\phi}_a$ are variational parameters and α can be thought of as a tilt or rotation angle of the ground state. The variational parameters satisfy $\hat{\phi}_1^2 + \hat{\phi}_2^2 + \hat{\phi}_3^2 = 1$ to ensure that the ground state is normalized, i.e. $(\Sigma_\alpha^{\pi^\pm})^\dagger \Sigma_\alpha^{\pi^\pm} = \mathbb{1}$. The thermodynamic potential Ω_0 is a function of the parameters $\hat{\phi}_a$ and the tilt angle α . After a straightforward calculation using the ansatz Eq. (14), Ω_0 becomes

$$\begin{aligned} \Omega_0 &= -f^2 m_{\pi^0}^2 \cos \alpha \\ &\quad - \frac{1}{2} f^2 (\mu_I^2 - \Delta m_{\text{EM}}^2) \sin^2 \alpha (\hat{\phi}_1^2 + \hat{\phi}_2^2). \end{aligned} \quad (15)$$

We notice that the energy is minimized for $\hat{\phi}_3 = 0$, so that neutral pions do not condense (the third component of the isospin is zero for a neutral pion). Thus $(\hat{\phi}_1^2 + \hat{\phi}_2^2) = 1$ and the energy is independent of the values of the parameters $\hat{\phi}_1$ and $\hat{\phi}_2$, this degeneracy reflects the breaking of the $U(1)_I$ symmetry in the pion-condensed phase. We can therefore choose $\hat{\phi}_2 = 1$ without loss of generality, which yields

$$\Sigma_\alpha^{\pi^\pm} = \cos \alpha \mathbb{1} + i \tau_2 \sin \alpha = e^{i\alpha \tau_2}, \quad (16)$$

$$\Omega_0 = -f^2 m_{\pi^0}^2 \cos \alpha - \frac{1}{2} f^2 \mu_{I,\text{eff}}^2 \sin^2 \alpha, \quad (17)$$

where $\mu_{I,\text{eff}}^2 = \mu_I^2 - \Delta m_{\text{EM}}^2$. The first term arises from the second term in the Lagrangian (1), while the second term comes from the second and third term. In minimizing the thermodynamic potential there is a competition between two terms in Eq. (17), where the first term prefers $\alpha = 0$

and the second term $\alpha = \frac{\pi}{2}$. The optimum value is found by minimizing Ω_0 , giving

$$\cos \alpha^* = \begin{cases} 1, & \mu_I^2 \leq m_{\pi^\pm}^2, \\ \frac{m_{\pi^0}^2}{\mu_{I,\text{eff}}^2}, & \mu_I^2 \geq m_{\pi^\pm}^2. \end{cases} \quad (18)$$

Thus there is a transition from the vacuum phase to a pion-condensed phase at $\mu_I^2 = m_{\pi^\pm}^2$. In the chiral limit, $\alpha^* = \frac{\pi}{2}$ and the quark condensate is rotated into a pion condensate for any nonzero μ_I .

We next consider three flavors. For $\mu_S = 0$, the two-flavor results and the fact that $\{\lambda_1, \lambda_2, \lambda_3\}$ form an $SU(2)$ algebra suggest that there is a transition to a pion-condensed phase at $\mu_I^2 = m_{\pi^\pm}^2$. Similarly, for $\mu_K^0 = 0$, we expect a transition to a phase with a charged kaon condensate at $\mu_{K^\pm}^2 = m_{K^\pm}^2$. Finally, for $\mu_{K^\pm} = 0$, a transition to a phase with a neutral kaon condensate takes place at $\mu_{K^0}^2 = m_{K^0}^2$. In the pion-condensed phase the $U(1)_I$ (and therefore also $U(1)_Q$) is broken. In the kaon condensed phases, either the $U(1)_Q$ or the $U(1)_K$ symmetry is broken. Without electromagnetic effects, these phases are superfluid. There is a single Goldstone boson associated with this breaking. If one includes them, the charged pion and kaon condensates are superconductors since the gauged $U(1)_Q$ is broken. There is no Goldstone boson in these phases as the Higgs mechanism eats this degree of freedom giving rise to massive photons with three polarizations. The form of the ground states is therefore

$$\Sigma_\alpha^{\pi^\pm} = e^{i\alpha \lambda_2}, \quad \Sigma_\beta^{K^\pm} = e^{i\beta \lambda_5}, \quad \Sigma_\gamma^{K^0/\bar{K}^0} = e^{i\gamma \lambda_7}, \quad (19)$$

where α , β , and γ are the tilt angles in the different cases and the superscript indicates the condensing meson. Generally, one should allow for the simultaneous condensation of two or more mesons. However, this is not supported by actual calculations. The relevant term from the static Lagrangian, $-\frac{1}{4} f^2 \langle [v_0, \Sigma_\alpha] [v_0, \Sigma_\alpha^\dagger] \rangle$ does not prefer multiple condensates [32].

In analogy with the two-flavor results, the transition points between the vacuum and Bose-condensed phases are determined by

$$\mu_I^2 = m_{\pi^\pm}^2, \quad \mu_{K^\pm}^2 = m_{K^\pm}^2, \quad \mu_{K^0}^2 = m_{K^0/\bar{K}^0}^2. \quad (20)$$

These equations define lines in the μ_I - μ_S plane and their intersection define the region of the vacuum phase. Outside this region, the Bose-condensed phase with the higher pressure wins.

In the pion-condensed phase, the pressure and isospin density are given by

$$p = -\Omega_0 \Big|_{\alpha=\alpha^*} = \frac{1}{2} f^2 \mu_{I,\text{eff}}^2 \left[1 - \frac{m_{\pi^\pm,0}^2}{\mu_{I,\text{eff}}^2} \right]^2, \quad (21)$$

$$n_I = -\frac{\partial \Omega_0}{\partial \mu_I} \Big|_{\alpha=\alpha^*} = f^2 \mu_I \left[1 - \frac{m_{\pi^\pm,0}^4}{\mu_{I,\text{eff}}^4} \right], \quad (22)$$

where we here and in the following have subtracted a constant such that $p = 0$ in the vacuum phase. The

strangeness density $n_S = -\frac{\partial \Omega_0}{\partial \mu_S} |_{\alpha=\alpha^*}$ vanishes. As $\mu_I \rightarrow m_{\pi^\pm}$ from above, the isospin density goes to zero continuously, which suggests that the transition to the vacuum state is of second order. In order to find the critical exponent, we construct a Landau-Ginzburg energy functional by expanding the thermodynamic potential around $\alpha = 0$. This yields, after omitting a constant term,

$$\Omega_0 = -\frac{1}{2}f^2[\mu_I^2 - m_{\pi^\pm}^2]\alpha^2 + \frac{1}{24}f^2[4\mu_I^2 - m_{\pi^\pm}^2 - 3\Delta m_{\text{EM}}^2]\alpha^4 + \dots \quad (23)$$

We define a critical chemical potential μ_I^c by the vanishing of the coefficient of the quadratic term. This yields $\mu_I^c = m_{\pi^\pm}$. Since the quartic term is positive when evaluated at the critical chemical potential, the transition is of second order as expected. Since $\alpha^* \propto [\mu_I^2 - \mu_I^{c2}]^{\frac{1}{2}}$, for small μ_I , the mean-field critical exponent is $\frac{1}{2}$.

In the K^\pm -condensed phase, the isospin and strangeness densities are given by

$$p = \frac{1}{2}f^2\mu_{K^\pm,\text{eff}}^2 \left[1 - \frac{m_{K^\pm,0}^2}{\mu_{K^\pm,\text{eff}}^2} \right]^2, \quad (24)$$

$$n_I = \frac{1}{2}f^2\mu_{K^\pm} \left[1 - \frac{m_{K^\pm,0}^4}{\mu_{K^\pm,\text{eff}}^4} \right], \quad (25)$$

$$n_S = f^2\mu_{K^\pm} \left[1 - \frac{m_{K^\pm,0}^4}{\mu_{K^\pm,\text{eff}}^4} \right], \quad (26)$$

where $\mu_{K^\pm,\text{eff}}^2 = \mu_{K^\pm}^2 - \Delta m_{\text{EM}}^2$. The result for the K^0/\bar{K}^0 condensed phases is obtained by making the substitutions $\mu_{K^\pm}^2 \rightarrow \mu_{K^0}^2$, $\mu_{K^\pm,\text{eff}}^2 \rightarrow \mu_{K^0}^2$, and $m_{K^\pm,0}^2 \rightarrow m_{K^0}^2$ in Eqs. (24)–(26).

Comparing the pressure of the phases with charged condensates, the transition line, on which the pressures (21) and (24) are equal, is determined by

$$\mu_{K^\pm,\text{eff}} = \frac{1}{2\mu_{I,\text{eff}}} \left(\mu_{I,\text{eff}}^2 - m_{\pi^\pm,0}^2 + \sqrt{(\mu_{I,\text{eff}}^2 - m_{\pi^\pm,0}^2)^2 + 4\mu_{I,\text{eff}}^2 m_{K^\pm,0}^2} \right). \quad (27)$$

A similar equation for the transition line between the neutral and charged kaon condensates can be obtained.

So far we have said nothing about f appearing in the various expressions for the pressure and the densities. In an $\mathcal{O}(p^4)$ analysis of the phase transition, similar to Eq. (23), f would be replaced by f_π if the transition is to a pion-condensed phase and f_K if the transition is to a kaon-condensed phase. It is therefore natural to identify f with the physical value for f_π or f_K depending on which phase we are studying. Identifying f with f_π also guarantees that the two and three-flavor results for the pion-condensed phase at $\mathcal{O}(p^2)$ are the same. In the next section, we therefore set $f = f_\pi$, whose experimental value is [38]

$$f_\pi = 92.2, \text{ MeV}. \quad (28)$$

In order to generate the phase diagram, we need the physical values for the pion and kaon masses taken from the Particle Data Group [38],

$$\begin{aligned} m_{\pi^0} &= 134.98 \text{ MeV}, & m_{\pi^\pm} &= 139.57 \text{ MeV}, \\ m_{K^\pm} &= 493.68 \text{ MeV}, & m_{K^0} &= 497.61 \text{ MeV}. \end{aligned}$$

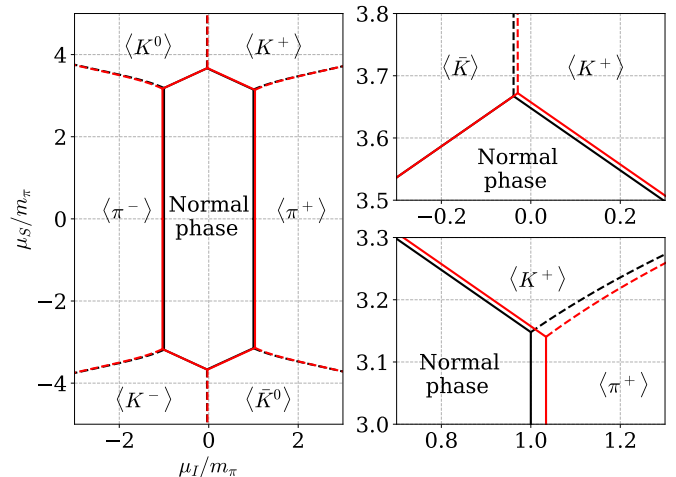


Figure 1: Phase diagram as predicted by χ PT in the μ_I - μ_S -plane. The black lines are results without electromagnetic interactions, while red lines are results including them. To the right, we have zoomed in on two of the triple points. Upper panel shows the intersection of the normal, neutral kaon condensed and charged kaon condensed phases, while the lower shows the intersection of the normal, pion condensed, and charged kaon condensed phases.

In Fig. 1, we show the phase diagram at $T = 0$ in the μ_I - μ_S plane. The black lines are the transition lines without electromagnetic interactions and the red lines are with electromagnetic interactions. The former was first obtained by Kogut and Toublan [22] with $m_u = m_d$. The transitions from the normal phase to a meson-condensed phase is always second order with mean-field exponents. The transitions are in the $O(2)$ universality class, as discussed above. The transitions between the various condensed phases are always first order and involves the competition between the order parameters between the different phases. As we cross the transition lines, the order parameters as well as the densities n_I and n_S jump discontinuously. For example, coming from the π^+ -condensed phase and crossing the the transition line to the K^+ -condensed phase, the strangeness density n_S jumps from zero to the value given by Eq. (26). The small offset of the dashed vertical lines is due to the mass difference between the charged and neutral kaons, which is both due to $\Delta m_{\text{EM}} \neq 0$, and $m_u \neq m_d$. These contributions, however, pull in opposite directions, as we see in the phase diagram. The contribution due to the difference in quark masses adds to the mass of the K^0/\bar{K}^0 meson, which is why the black transition line between the kaon condensate is to the left of the $\mu_I = 0$ line, while the electromagnetic contribution adds to the mass of the charged kaon, which is why the red line is between these two lines. The partition function in the

normal phase is independent of the two chemical potentials μ_I and μ_S , which is the Silver Blaze property [44]. It implies that all the thermodynamic functions are constant, for example that the pressure and the charge densities vanish. Similarly, the partition function in the condensed phases is independent of one of the chemical potentials μ_I or $\pm\frac{1}{2}\mu_I + \mu_S$, implying that $n_S = 0$, $n_{K^\pm} = 0$, or $n_{K^0/\bar{K}^0} = 0$, respectively.

The phase diagram has been mapped out under the assumption that the chemical potentials are small so that χ PT is inside its region of validity. The expansion parameter is $M/4\pi f$, where M is a mass or a chemical potential. An expansion parameter of $\frac{1}{2}$ corresponds to $M \approx 565$ MeV. Another constraint on the region of validity of χ PT is the appearance of new resonances not in the model. The first new resonance to appear is the ρ -meson, at $M \approx 770$ MeV. A natural question to ask is: what happens at larger values of μ_I and μ_S . For asymptotically large values of μ_I , asymptotic freedom implies that quarks are weakly interacting and a description in terms of these degrees of freedom applies [19, 20]. One-gluon exchange gives rise to an attractive channel, rendering the Fermi surface unstable to the formation of Cooper pairs of \bar{u} and d quarks or \bar{d} and u depending on the sign of μ_I . The resulting BCS phase is characterized by the same order parameter as the pion-condensed phase [19, 20].

3. Pion stars

Describing a pion star using the perfect fluid approximation as done for neutron stars, requires an equation of state. For an ideal Bose gas at zero temperature, all the bosons are in the zero-momentum state, the pressure is vanishing, and there is no equation of state [39]. In contrast to neutron stars, where the Pauli principle gives rise to a quantum pressure at $T = 0$, we need interactions in the bosonic case. In the pion-condensed phase, the mean-field pressure is given in Eq. (21), which vanishes for $f = f_\pi = 0$. Using p and ϵ to describe matter, the Tolman-Oppenheimer-Volkov (TOV) equation for a spherically symmetric star follows directly from Einstein's fields equation. The continuity equation and the TOV equation for a spherically symmetric star are

$$\frac{dm}{dr} = 4\pi r^2 \epsilon(r), \quad (29)$$

$$\frac{dp}{dr} = -\frac{G\epsilon(r)m(r)}{r^2} \left[1 + \frac{p(r)}{\epsilon(r)} \right] \times \left[1 + \frac{4\pi r^2 p(r)}{m(r)} \right] \left[1 - \frac{2Gm(r)}{r^2} \right]^{-1}. \quad (30)$$

The TOV equation is the general-relativistic generalization of the corresponding equation in Newtonian physics, which is derived from imposing hydrostatic equilibrium throughout the star. The two equations above are coupled and involve three unknowns, namely the pressure $p(r)$, the energy density $\epsilon(r)$, and the gravitational mass inside a shell

of radius r , $m(r)$. We therefore need the equation of state $p(\epsilon)$ to close the system. The pressure is a function of one or more chemical potentials depending on the composition of the star. Imposing electric charge neutrality and assuming chemical equilibrium yield a number of constraints among them and one ends up with a single free chemical potential, for example μ_I . The pressure and the energy density can then be parameterized uniquely by it.

The energy density is given by a Legendre transform of the pressure,

$$\epsilon = -p + \sum_i n_i \mu_i, \quad (31)$$

where the sum i is over all relevant chemical potentials.

We first discuss a pure pion star with the thermodynamic quantities at $\mathcal{O}(p^2)$ and set for simplicity $\Delta m_{\text{EM}}^2 = 0$ in Eqs. (32)–(35) below. For the pion-condensed phase, we can find the energy density using Eqs. (21) and (22). Expressing ϵ as a function of p , we obtain the EoS

$$\epsilon(p) = -p + 2\sqrt{p(p + 2f_\pi^2 m_{\pi^\pm,0}^2)}. \quad (32)$$

In the ultrarelativistic limit $\mu_I \rightarrow \infty$, the EoS reduces to $\epsilon = p$, which is a polytrope with index $n = \infty$ or $\gamma = 1$. In the opposite limit, we write the isospin chemical potential as $\mu_I = m_{\pi^\pm,0} + \mu_{\text{NR}}$, where $\mu_{\text{NR}} \ll m_{\pi^\pm,0}$ is the non-relativistic chemical potential. One can then show that

$$p = 2f_\pi^2 \mu_{\text{NR}}^2, \quad (33)$$

$$n_I = 4f_\pi^2 \mu_{\text{NR}}, \quad (34)$$

$$\epsilon = m_{\pi^\pm,0} n_I + \frac{1}{8f_\pi^2} n_I^2. \quad (35)$$

This yields the equation of state is $p = K\epsilon^2$, i.e. it is a polytrope with polytropic index $n = 1$ and constant $K^{-1} = 8m_{\pi^\pm}^2 f_\pi^2$. It is also a polytrope with $n = 1$ for $\Delta m_{\text{EM}}^2 \neq 0$, but now with $K^{-1} = 8m_{\pi^\pm}^4 f_\pi^2 / m_{\pi^0}^2$. The pressure and energy density are those of a weakly interacting nonrelativistic Bose gas with an s -wave scattering length $a = \frac{m}{16\pi f_\pi^2}$ in the mean-field approximation, first obtained by Bogoliubov [43].² For stars with a sufficiently low central pressure, we expect that the EoS of a dilute Bose gas is a good approximation. Moreover, if $\epsilon(r) \gg p(r)$ and $r \gg 2Gm(r)$, the TOV equation reduces to the Newtonian equation for hydrostatic equilibrium, namely the Lane-Emden equation. It is expected that this is also a good approximation for sufficiently low-mass stars. Solving the Lane-Emden equation for $\gamma = 2$, one finds that the radius R is independent of its mass, i.e. it corresponds to a vertical line in the mass-radius diagram.³ The radius in

²To obtain the energy density of a dilute Bose gas, we subtract the leading term $m_{\pi^\pm,0} n_I$ associated with the rest mass energy.

³This limit is analogous to the Chandrasekhar limit for white dwarfs, where its radius is independent if its mass attains its maximum value, approximately $1.4M_\odot$.

the Newtonian limit is given by

$$R = \pi \sqrt{\frac{K}{2\pi G}}. \quad (36)$$

This is shown in Fig. 2, where we plot the mass-radius relation in different approximations for a pure pion star without electromagnetic interactions.

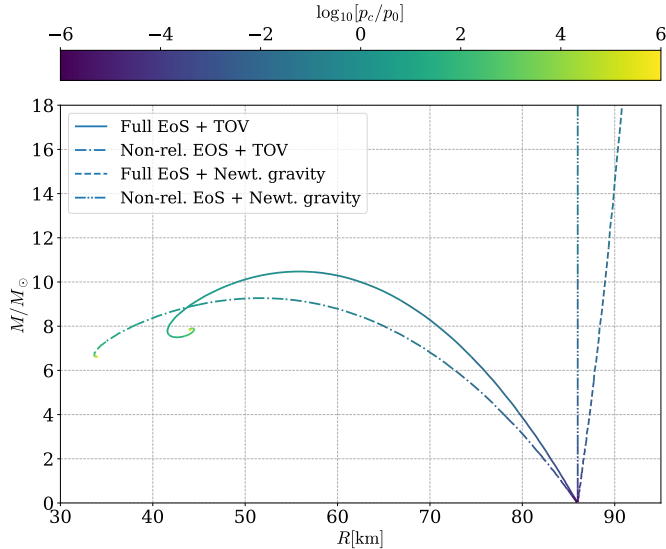


Figure 2: Mass-radius relation for a pure pion star without electromagnetic interactions in different approximations. See main text for details.

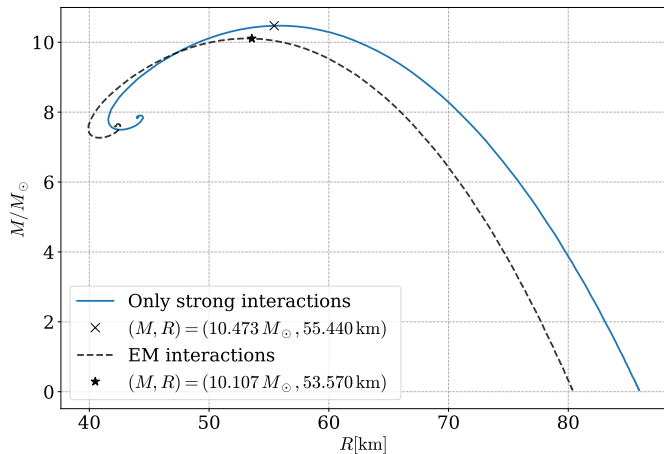


Figure 3: Mass-radius relation for a pure pion star. See main text for details.

In Fig. 3, we show the mass-radius relation for a pure pion star. The solution to the TOV equation without electromagnetic interactions is given by the solid line, where the stable stars are to right of the maximum mass indicated by a cross. The maximum mass is $M_{\max} = 10.47M_{\odot}$ and the corresponding radius is $R = 55.4$ km. The mass-radius relation including electromagnetic interactions is given by the black dashed line in Fig. 3. The maximum

mass is now $10.1M_{\odot}$ with a radius of 53.6 km. The maximum radius for vanishing mass is $R_{\max} = 86$ km. If we include electromagnetic effects, the maximum radius is reduced to $R_{\max} = 80$ km. These numerical results are in excellent agreement with the limit Eq. (36).

We next discuss electric charge neutrality. Since condensed pions are electrically charged, a pure pion star has a macroscopic electric charge. However, due to the Coulomb repulsion among the pions, there is an enormous energy cost of having bulk matter that is not electrically neutral [42]. We will therefore impose local electric charge neutrality by adding a background charge of leptons. This amounts to requiring

$$n_I - \sum_l n_l = 0, \quad (37)$$

where the sum is over lepton species l . Chiral perturbation theory can be extended to include the light leptons as dynamical degrees of freedom [45]. The $\mathcal{O}(p^2)$ -term one should add to the Lagrangian Eq. (1) is

$$\mathcal{L}_2 = \sum_l [\bar{l}(i\cancel{\partial} - \mu_l\gamma_0 + e\cancel{A} - m_l)l + \bar{\nu}_{lL}(i\cancel{\partial} - \mu_{\nu_l}\gamma_0)\nu_{lL}], \quad (38)$$

where we include the electron and the muon in the sum, m_l is the lepton mass, μ_l and μ_{ν_l} are the corresponding chemical potentials. The neutrinos are massless, $m_{\nu_l} = 0$, and the subscript L indicates that there are only left-handed neutrinos. In the power counting scheme adopted in Ref. [45], a fermion bilinear and lepton mass both count as $\mathcal{O}(p)$. Below we include the leading contributions to the pressure and energy density, which according to the above counting scheme are $\mathcal{O}(p^4)$. It is therefore not consistent to include strong and electromagnetic interactions among the pions to $\mathcal{O}(p^2)$ and the leptons to $\mathcal{O}(p^4)$. We therefore include the $\mathcal{O}(p^4)$ corrections from the pions in the pressure, isospin density, and energy density. Details of the calculations can be found in Ref. [32] or in a forthcoming paper [33]. Moreover, the $\mathcal{O}(p^4)$ electromagnetic effects are prohibitively difficult to calculate, but since we are mainly interested in the comparison with the lattice simulations, we do not need them anyway.

A lepton with chemical potential $\mu_l > m_l$ contributes to the pressure and energy density as

$$p_l = \frac{2m_l^4}{3(4\pi)^2} \left[(2x_l^3 - 3x_l)\sqrt{1+x_l^2} + 3\text{arcsinh } x_l \right], \quad (39)$$

$$\epsilon_l = \frac{2m_l^4}{(4\pi)^2} \left[(2x_l^3 + x_l)\sqrt{1+x_l^2} - \text{arcsinh } x_l \right], \quad (40)$$

where $x_l = \frac{\sqrt{\mu_l^2 - m_l^2}}{m_l}$ is the dimensionless ratio of the Fermi momentum and the mass of the lepton. The contribution to the charge density from a lepton is

$$n_l = \frac{\partial p}{\partial \mu_l} = \frac{16}{3(4\pi)^2} (\mu_l^2 - m_l^2)^{\frac{3}{2}}. \quad (41)$$

Considering again the nonrelativistic limit for a fermion, the standard results for the lepton pressure and energy density are

$$p_l = \frac{16m_l^4}{15(4\pi)^2}(\mu_l^2 - m_l^2)^{\frac{5}{2}}, \quad \epsilon_l = m_{\pi^\pm} n_l, \quad (42)$$

which leads to the equation of state $p_l = K\epsilon_l^{\frac{3}{5}}$. The neutrinos are massless so p and ϵ are given by their ultra-relativistic limit, including a factor of $\frac{1}{2}$ due to the absence of right-handed neutrinos and left-handed antineutrinos,

$$p_{\nu_l} = \frac{2\mu_{\nu_l}^4}{3(4\pi)^2}, \quad \epsilon_{\nu_l} = \frac{2\mu_{\nu_l}^4}{(4\pi)^2}. \quad (43)$$

Pions are unstable particles that mainly decay via weak interactions. The dominant decay mode is $\pi \rightarrow \mu + \nu_\mu$. In chemical equilibrium, the reactions rates of $\pi^+ \rightarrow l^+ + \nu_\mu$ and $\pi^- \rightarrow l^- + \bar{\nu}_\mu$ are the same, implying the relation

$$\mu_I = \mu_l - \mu_{\nu_l}, \quad (44)$$

where l is either an electron or a muon. Although we ignore the neutrino masses in the analysis, the nonzero masses imply a relation between their chemical potentials via neutrino oscillations. Chemical equilibrium among the two species yields

$$\mu_{\nu_e} = \mu_{\nu_\mu}, \quad (45)$$

or equivalently $\mu_e = \mu_\mu$. We have six chemical potentials, $\mu_I, \mu_Q, \mu_e, \mu_\mu, \mu_{\nu_e}$, and μ_{ν_μ} . Chemical equilibrium and charge neutrality reduce this number to a single independent chemical potential.

We note that at the transition when $\mu_I = m_{\pi^\pm}$, the lepton density also vanishes due to the charge neutrality constraint (37). However, chemical equilibrium, Eq. (44), implies that the neutrino chemical potential and consequently the neutrino density is nonzero at the transition point, i.e. on the surface of the pion star. The star therefore has a neutrino atmosphere with an EoS $\epsilon = 3p$.

In the absence of electromagnetic interactions, we take the physical mass of the neutral pion and kaon as our common meson masses. The masses of the leptons are also taken from Ref. [38]

$$m_e = 0.51 \text{ MeV}, \quad m_\mu = 105.6 \text{ MeV}. \quad (46)$$

In order to compare with lattice simulations, we also use the set in Ref. [14]. The central values are given by

$$m_\pi = 131 \text{ MeV}, \quad m_K = 481 \text{ MeV}, \quad f_\pi = 90.8 \text{ MeV}. \quad (47)$$

In Fig. 4, we show the mass-radius for pion stars including leptons and neutrinos. The blue band is obtained from lattice simulations including the statistical and systematic errors in the EoS. The black solid and dashed lines are obtained from the $\mathcal{O}(p^2)$ EoS from χ Pt using the PDG and lattice values for the meson masses, respectively. The red

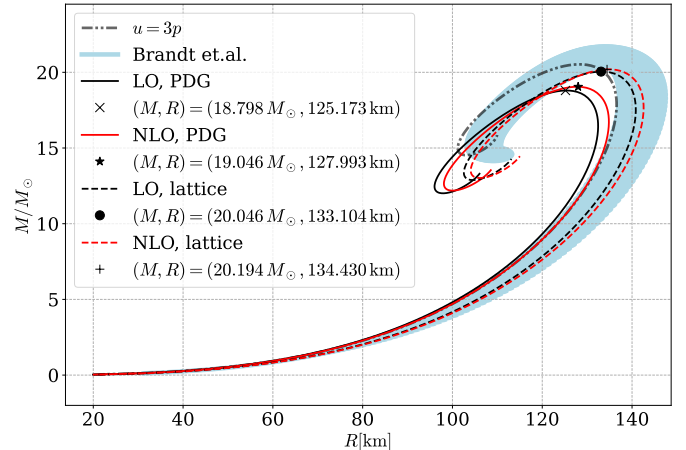


Figure 4: Mass-radius relations for a pion star for the different cases as indicated by the legends. Electromagnetic interaction are not included. The dashed lines are results using the EoS obtained from lattice calculations [12].

solid and dashed lines are obtained from the $\mathcal{O}(p^4)$ EoS and the same sets of meson masses. The results show that the mass-radius relations are rather sensitive to the masses and decay constant. This change can mostly be understood as a scaling of the variables in the TOV equation. As we will discuss further, the EoS is dominated by the neutrinos, so the most important mass scale is $p_{\min} \propto f_\pi^2 m_\pi^2$, where p_{\min} is the pressure on the surface of the star. Scaling the pressure and energy density in the TOV equation by t^2 leads to a scaling of M, R by t^{-1} , so we expect both mass and radius to be proportional to $1/m_\pi f_\pi$. Using the lattice constants, this quantity is around 5% larger than using the PDG constants, which accounts for most of the difference in 3.

Moreover, the results for the $\mathcal{O}(p^2)$ and $\mathcal{O}(p^4)$ curves are very close. The quantity $\frac{\mu_\pi}{m_\pi} - 1$ is equal to 2.0×10^{-2} at $\mathcal{O}(p^2)$ and 1.8×10^{-2} at $\mathcal{O}(p^4)$ at the center for the heaviest star, denoted by the crosses. This corresponds to the largest values of μ_I on the entire branch. In this region the corrections to the thermodynamic quantities are small suggesting that we can reliably use χ Pt to calculate the properties of pion stars. As noted above, at the surface of the star, $\epsilon = 3p$. Chemical equilibrium and charge neutrality imply that $\mu_e = \mu_\mu = m_e$ and therefore $\mu_{\mu_e} = \mu_{\mu_\nu} = m_{\pi^\pm,0} + m_e$. This yields the pressure on the surface $p_{\min} = \frac{4}{3(4\pi)^2} (m_{\pi^\pm,0} + m_e)^4$.

The equation of state in the charge neutral pion condensate is well approximated by $\epsilon = 3p$, especially for low pressures, as the neutrino contribution dominates. In Fig 4, we have included the results of solving the TOV equation with this EoS, and a surface pressure $p = p_{\min}$. The result is the grey dashed curve in Fig. 4, demonstrating that the EoS is dominated by the neutrinos if the star is not too compact.

A further investigation of pion stars requires a more complete understanding of their evolution and instabili-

ties. A necessary requirement for the stability of stars against spherical perturbations is the increase of their mass as the central pressure increases [40],

$$\frac{dM}{dp_c} \geq 0. \quad (48)$$

Brandt et al. showed, as expected, that pion stars including leptons and neutrinos are stable for central pressures below that of the maximum mass configuration [14]. In addition to perturbations, an important component of the stability of pion stars is the decay rate of its constituent particles. As the pion star is modeled at zero temperature, the decay of the pion condensate into neutrinos and charged leptons will be Pauli blocked. The neutrino atmosphere, however, is not gravitationally bound as we consider neutrinos massless. This will lead to the depletion of the lepton number at the edge of the star.

4. Acknowledgements

The authors would like to thank B. Brandt, G. Endrődi, and S. Schmalzbauer for useful discussions as well as their lattice data for the mass-radius relation of pion stars [41].

References

- [1] D. Bailin and A. Love, *Phys. Rept.* **107**, 325 (1984).
- [2] K. Rajagopal and F. Wilczek, *At the frontier of particle physics*, Vol. 3 (World Scientific, Singapore, p 2061) (2001).
- [3] M. G. Alford, A. Schmitt, K. Rajagopal, and T. Schäfer, *Rev. Mod. Phys.* **80**, 1455 (2008).
- [4] K. Fukushima and T. Hatsuda, *Rept. Prog. Phys.* **74**, 014001 (2011).
J. B. Kogut and D. Toublan, *Phys. Rev. D* **64** (2001) 034007 (2001).
- [5] J. B. Kogut and D. K. Sinclair, *Phys. Rev. D* **66**, 014508 (2002).
- [6] J. B. Kogut and D. K. Sinclair, *Phys. Rev. D* **66** 034505 (2002).
- [7] J. B. Kogut and D. K. Sinclair, *Phys. Rev. D* **70** 094501 (2004).
- [8] D. K. Sinclair and J. B. Kogut, *PosLat 2006* **147** (2006).
- [9] D. K. Sinclair, J. B. Kogut, *PoS LAT 2007* **225** (2007).
- [10] B. B. Brandt and G. Endrődi, *PoS LATTICE 2016*, 039 (2016).
- [11] B. B. Brandt, G. Endrődi, and S. Schmalzbauer, *EPJ Web Conf.* **175**, 07020 (2018).
- [12] B. B. Brandt, G. Endrődi, and S. Schmalzbauer, *Phys. Rev. D* **97**, 054514 (2018).
- [13] B. B. Brandt and G. Endrődi *Phys. Rev. D* **99**, 014518 (2019)
- [14] B. B. Brandt, Endrődi, E. S. Fraga, M. Hippert, J. Schaffner-Bielich, and S. Schmalzbauer *Phys. Rev. D* **98**, 094510 (2018).
- [15] M. M. Middeldorf-Wygas, I. M. Oldengott, D. Bödeker, D. J. Schwarz, *Phys.Rev.Lett.* 121 (2018) 20, 201302.
- [16] M. M. Middeldorf-Wygas, I. M. Oldengott, D. Bödeker, D. J. Schwarz, e-Print:2009.00036 [hep-ph].
- [17] V. Vovchenko, B. B. Brandt, F. Cuteri, G. Endrődi, F. Hajarim, and J. Schaffner-Bielich *Phys. Rev. Lett.* **126**, 012701 (2021).
- [18] Supplemental material of Ref. [17].
- [19] D. T. Son and M. A. Stephanov, *Phys. Rev. Lett.* **86**, 592 (2001).
- [20] D. T. Son and M. A. Stephanov, *Phys. Atom. Nucl.* **64**, 834 (2001).
- [21] K. Splittorff, D. T. Son, M. A. Stephanov, *Phys. Rev. D* **64**, 016003 (2001).
- [22] J. B. Kogut and D. Toublan, *Phys. Rev. D* **64** (2001) 034007 (2001).
- [23] S. Carignano, A. Mammarella, and M. Mannarelli, *Phys. Rev. D* **93**, 051503 (2016).
- [24] S. Carignano, L. Lepori, A. Mammarella, M. Mannarelli, and G. Pagliaroli *Eur. Phys. J. A* **53**, 35 (2017).
- [25] P. Adhikari, J. O. Andersen, and P. Kneshcke, *Eur. Phys. J. C* **79**, 874 (2019).
- [26] P. Adhikari, J. O. Andersen, and M. A. Mojahed, *Eur. Phys. J. C* **81**, 449 (2021).
- [27] M. S. Grønli and T. Brauner, *Eur. Phys. J. C* **82**, 354 (2022).
- [28] J. Gasser and H. Leutwyler, *Ann. Phys.* **158**, (142) (1984).
- [29] J. Gasser and H. Leutwyler, *Nucl. Phys. B* **250**, 465 (1985).
- [30] M. Mannarelli, *Particles* **2**, 411 (2019).
- [31] H. Abuki, T. Brauner, H. J. Warringa, *Eur. Phys. J. C* **64**, 123 (2009).
- [32] J. O. Andersen and Martin K. Johnsrud, in preparation.
- [33] Martin K. Johnsrud, Master thesis, NTNU 2022. Thesis and code available at <https://github.com/martkjoh/master>.
- [34] G. Ecker, J. Gasser, A.Pich, and E. De Rafael, *Nuclear Physics B* **321**, 311 (1989).
- [35] R. Urech, *Nucl. Phys. B* **433**, 234 (1995).
- [36] M. Knecht and R. Urech, *Nucl. Phys. B* **519**, 329 (1998).
- [37] U.-G. Meißner, G. Müller and S. Steininger, *Phys. Lett. B* **406**, 154 (1997).
- [38] P.A. Zyla *et al.* [Particle Data Group],
- [39] P. Jetzer, *Phys. Rept.* **220**, 163 (1992).
- [40] N. K. Glendenning, *Compact Stars: Nuclear Physics, Particle Physics and General Relativity, 2nd edition* (2000).
- [41] B. B. Brandt, G. Endrődi, and S. Schmalzbauer, private communication.
- [42] A. Schmitt, *Lect. Notes Phys.* **811**, 1 (2010).
- [43] N. N. Bogoliubov, *J. Phys. (Moscow)* **11**, 23 (1947).
- [44] T. D. Cohen and S. Sen, *Nucl. Phys. A* 942, 39 (2015).
- [45] M. Knecht, H. Neufeld, H. Rupertsberger, and P. Talavera *Eur. Phys. J. C* **12**, 469 (2000).